






Disassembly and Structural Reuse Potential of Steel-Timber Shear Connections with Screws

Dan V. Bompá¹ , Viorel Ungureanu² , Ahmed Y. Elghazouli^{3,4} ,
and Ahamed Afsal¹

¹ School of Sustainability, Civil and Environmental Engineering, University of Surrey,
Guildford, UK

d.bompa@surrey.ac.uk

² Department of Steel Structures and Structural Mechanics, Politehnica University
Timisoara/Technical Science Academy of Romania, Timișoara, Romania

³ Department of Civil and Environmental Engineering, Imperial College London, London, UK

⁴ Department of Civil and Environmental Engineering, Hong Kong Polytechnic University,
Hong Kong, China

Abstract. The paper evaluates the disassembly capability and reuse potential of steel-timber shear connections. Experiments involving double shear configurations with coach screws of three diameters are detailed. Monotonic tests were first performed for each configuration to evaluate the stiffness, strength, and ductility. Counterparts were then tested under ten loading-unloading cycles, to 40% of the capacity obtained from the monotonic tests, to evaluate stiffness degradation characteristics, screw deformations, and cross-laminated timber (CLT) panel damage. After disassembly and measurements, the specimens were reassembled and tested up to failure. The measurements indicated that the secant stiffness enhances after the first loading cycle and is then largely constant to the tenth cycle. After disassembly, the screws had permanent deformations, and the timber panels indicated limited damage during the cyclic loading. The reassembled specimens had similar stiffness, strength, ductility, and failure modes as the monotonic test specimens. Based on test measurements, both the steel profile and the CLT panels have full structural reusability. The test results can be used as a measure for quantification of the structural reuse potential through an index that can be incorporated into established building circularity indicators.

Keywords: Steel-timber · Disassembly capability · Reuse potential · Circularity

1 Introduction

To achieve established reduction targets by 2030 and net-zero by 2050, innovative building systems such as steel-timber hybrids (STH) are needed. Building structures incorporating timber have the potential to contribute to reducing embodied carbon by 60%, storing sequestered carbon by up to 400% as well as can be designed for disassembly, compared with conventional concrete structures [1]. Steel-timber and timber-concrete solutions for multi-storey buildings highlighted the synergetic behaviour of the two

materials [2]. Whilst timber-concrete hybrids were the subject of many studies, STH systems, particularly for taller structures, were less investigated.

Recently built six-storey educational and ten-storey residential STH buildings highlighted the benefits of such systems for reduced construction time (offsite manufacturing, design for assembly) and enhanced environmental sustainability (less embodied carbon and potential for disassembly and reuse at the end of life) compared to other composite or conventional building systems [3]. Steel-timber hybrid structures are considered lightweight systems suitable for prefabricated modular buildings [4] and consist mainly of steel columns with steel or timber beams with CLT or LVL slabs [5, 6]. To achieve composite action, steel-timber floor shear connections can be either dry, by using mechanical fasteners, or wet, requiring the use of epoxy-based resins. The latter offers enhanced initial bending stiffness, yet the ultimate behaviour is associated with brittle failures compared to dry connections [7]. The use of wet connections may impair the disassembly at the end of life, rendering them less circular.

Circularity is a systemic approach that aims to eliminate waste and optimise resource utilisation. This is typically measured through indicators that provide information about the extent to which resources are used efficiently, recycled, and kept within a closed loop. Within the main principles of circularity in buildings, slowing the resource loops refers to decelerating the resource flows by improving their utilisation and expanding their valuable lifespan. This refers to design for durability, long life and life extension, for adaptability and reversibility, reuse and repurpose. Dry shear connections in STH floors align with these principles of circularity, enabling disassembly and reuse and repurpose of the components with minimal or no loss of mechanical properties.

Experimental and numerical studies on conventional shear connections for STH floors exist, focussing primarily on structural performance. These include screwed, bolted, or grouted connections that were tested either under monotonic or cyclic loading to failure. In line with circularity drivers, evaluation of the constructability and disassembly and reuse potential is essential but has not been evaluated. This paper evaluates the disassembly capability of screwed steel-timber shear connections, tested under in-service cyclic loading, as well as the reassembly and structural reuse potential through testing. The experiments involved double-shear configurations with coach screws. After describing the testing methods and the main results, a qualitative discussion of the disassembly and reuse is undertaken.

2 Response of Steel-Timber Shear Connections

In steel timber shear connections, failure can typically occur by four governing modes. As illustrated in Fig. 1, the mechanisms developing in the shear connections are through: (1) screw shear failure when the shear resistance of the connector is relatively weak in comparison with the timber element, (2) timber crushing with elastic behaviour of the connector, with this response occurring when the connector is strong in relation to the wood materials; and mixed-mode failures such as (3) with connector plastic hinging and timber crushing, and (4) double hinging in the connector with timber crushing.

Tests on three types of self-tapping screws in STH shear connections exhibited ductile failure mode with post-elastic bending deformation and CLT panel crushing

[8]. Connections loaded perpendicular to the grain had higher strength, while those loaded parallel had greater stiffness. Longer fasteners increased connection strength. Closer spacing of fasteners decreased stiffness and connection strength. Push-off tests showed increased shear capacities with inclined screws but decreased stiffness, compared to perpendicularly installed screws [9]. The use of tapper washers increased stiffness but also caused shear damage. Screws with long shanks were recommended for good ductility, and multiple rows of screws resulted in decreased strength per connector.

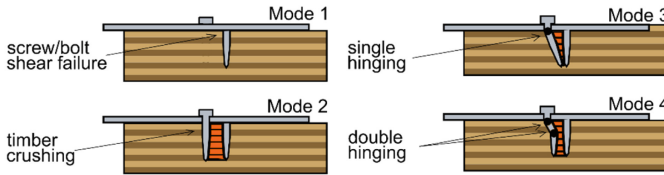


Fig. 1. Failure modes in steel-timber shear connections with screws.

Dry connections made using coach screws in steel-CLT shear connections demonstrated rather ductile behaviour [6]. Comparative wet connections had higher strengths and stiffnesses, but an overall more brittle response due to panel separation or glue fracture. Parallel to the grain, the load-slip responses were close to elastic-perfectly plastic, while in the perpendicular direction, there was hardening due to timber densification. The strength was higher perpendicular to the grain, but service stiffness was lower due to the lower elastic modulus of timber in that direction. Quasi-static cyclic tests were performed on steel-timber specimens with various types of shear connections, such as vertical or inclined self-tapping screws, epoxy resins, and glued steel slotted plates, among others [4]. As expected, dry connections with screws had lower strength and stiffness compared to systems with slotted plates and epoxies.

3 Experimental Assessment

3.1 Materials

The engineered timber employed in this study was a Cross-Laminated Timber (CLT) composed of three layers with a nominal thickness of 95 mm and a strength category of C24 spruce lamellae (softwood). Each layer was orthogonal to the subsequent at a 90-degree angle. Each layer measured approximately 32 mm in thickness, and the layer alignment was as follows: 32L/32 T/32L, where L indicates the longitudinal orientation and T the transverse orientation. The outer layers were aligned so that the load is applied in the direction parallel to the grain. For the push-out tests the CLT panels were 300 mm × 400 mm × 95 mm (width × height × thickness). Compression assessments were performed parallel to the grain on five CLT samples with an average size of 150 mm × 300 mm × 95 mm (width × height × thickness).

The specimens, shown in Fig. 2, were made up of two CLT panels that are linked to the flanges on both sides of an S235 hot-rolled open section with a characteristic yield

strength of 235 MPa. The dimensions of the profile were: section depth $h = 161.8$ mm, section depth $b = 154.4$ mm, flange thickness of $t_f = 11.5$ mm, and web thickness of $t_w = 8.0$ mm. To connect the CLT panels to the steel beam, coach screws with hexagon head, made of hardened steel and complementary washers were used. The screws were of 8 mm, 10 mm and 12 mm diameters, each respective diameter with 80 mm length, grade 4.8, 340 MPa nominal yield strength and 420 MPa nominal ultimate strength.

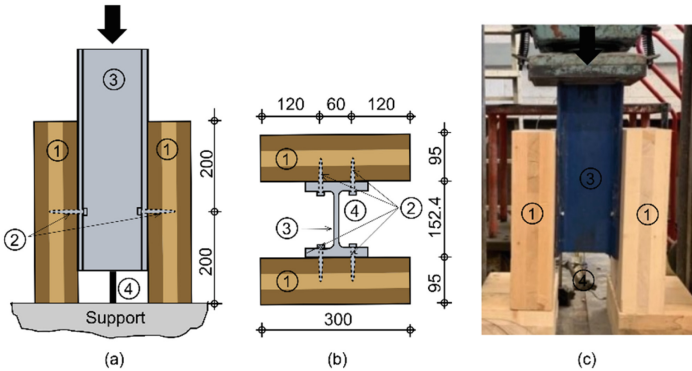


Fig. 2. Details of the test specimens: a) schematic front view, b) top view, c) view of a test specimen (legend: (1) CLT panel, (2) screws, (3) steel profile, (4) transducer, arrow indicates reaction point).

3.2 Specimens

A total of twelve specimens were prepared for testing. These included six for the monotonic test (M) and six for the reuse potential test (R). The former tests involved testing to failure, whilst the later involved repeated cyclic loading, specimen disassembly and measurements, reassembly with new screws and testing to failure. For each test, two samples were used for each coach screw diameter to enable a comparison of the results. The specimens were identified based on their respective screw diameters, resulting in the specimen labels following the format X-Y-z, in which X is the loading protocol (X = M, R for monotonic and reuse potential, respectively), Y is the screw diameter (Y = 8, 10, or 12 mm), and z is for the specimen sequence (z = a, b). For example, specimen name R-12-b represents the case of the second specimen tested under the suggested reuse potential protocol, which used 12 mm screws.

The CLT was available in the form of full-sized boards with varying dimensions, which were cut in the workshop into 24 panels to the above-mentioned sizes. The supporting edge of each panel was smoothed with a planer to prevent any instability and to encourage uniform contact with the testing platform and eliminate any unequal load distribution throughout testing. For consistency, a 60 mm distance between the axis of the two screws was considered for all specimens. Transversely, 120 mm and longitudinally, 200 mm, were considered between the edge of the panel and the screws.

Prior to assembly, holes of half the size of the corresponding net screw diameters were predrilled in the timber panel to facilitate screw installation. The panels were attached to the steel column flanges using two coach screw connectors, washers, and a torque tool, as shown in Fig. 2. The torque tool was used to ensure the same level of tightness for all samples. Washers were used to enhance the contact area of the connectors with the panels, to ensure a smoother stress distribution at the connection. As seen in Fig. 2 the connectors were completely integrated in the panels, leaving no exposed smooth shank or inclination. The panels were orientated for the load to act out parallel to the grain direction of the outer panel.

3.3 Testing Procedures

As mentioned above, twelve tests were carried out, equally divided into monotonic tests to failure (M) and reuse potential tests (R), as shown in Fig. 3. The tests were carried out to understand the overall response, the disassembly capability and structural reuse potential. For this, a 1MN Avery Instron testing machine with a ball seating was used. The latter had the purpose to prevent development of any out-of-plane deformation that would induce bending moment in the connection. In the monotonic tests (M), and the post-reassembly phase of the reuse potential tests (R) a displacement rate of 1 mm/min was applied before deviation of linearity in the load-slip ($F-\delta$) curve. This rate was then increased to 5 mm/min to failure. The $F-\delta$ curves and main structural parameters were recorded during the tests by the machine and additional transducers.

For the reuse potential tests (R), the average maximum strength of the corresponding monotonic tests (M) was used. The specimens were subjected to cycles starting from zero to 40% of the result obtained from the monotonic test. This complete cycle of loading and unloading was conducted ten times consecutively. After completion of the ten cycles, the specimen was removed from the testing rig and disassembled. The specimen was secured to prevent any movement during the disassembly process using clamps or vice grips. The screws were then loosened with a wrench due to limited accessibility. For deeper steel sections, electrical screwdrivers or similar tools can be used. Once the screws were sufficiently loosened, these were removed carefully to prevent any potential damage to the CLT panel or the steel sections. The damage length occurred in the timber panel was then measured with a ruler. Finally, the steel and timber elements were inspected separately for any visible damage.

New screws were installed into the pre-existing holes of the same specimen to evaluate the residual properties of the connection post-disassembly. After reassembly, as noted, the same procedure as for monotonic tests was applied. The load and slip were recorded by the machine and the additional transducer by a data logger. These data permit the evaluation of the main residual mechanical properties such as stiffness, strength, and ductility of the connection. In direct correlation with the monotonic tests, these give an indication of the structural reuse potential of the investigated connections.

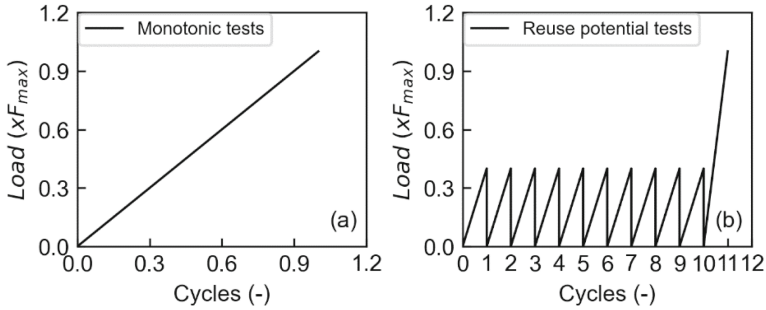


Fig. 3. Loading procedures: a) monotonic tests, b) reuse potential tests.

4 Test Results

Tables 1 and 2 and Figs. 4, 5, 6, 7 and 8 depict the main test results from the monotonic and the reuse potential tests. These include load-slip (F - δ) curves, failure kinematics, and the main response parameters. These are the secant stiffness at 40% ($k_{0.4}$) and 60% ($k_{0.6}$) of maximum capacity (F_{max}), the yield load (F_y), slip at yield (δ_y), ultimate slip (δ_u) corresponding to either slip at failure or 20% decrease from F_{max} , and a slip ductility ratio ($\mu_\delta = \delta_u/\delta_y$). Additionally, for the reuse potential tests, $k_{I,0.4}$, $k_{I,0.4}'$, corresponding to the secant stiffness at 40% F_{max} for the first cycle, the tenth cycle prior to disassembly, respectively, parameters $k_{II,0.4}$ and $k_{II,0.6}$ for the reassembled case are also reported.

4.1 Monotonic Tests

Figure 4 show the F - δ curves for the tested specimens. The M-8 specimens experienced failure without demonstrating any hardening. The secant stiffness $k_{0.4}$ and $k_{0.6}$ varied between 2.85–3.00 kN/mm. Specimen M-8-1 exhibited a yield strength F_y of 19.1 kN, and a corresponding slip δ_y of 6.5 mm, while its peak strength F_{max} reached 26.6 kN with an ultimate slip δ_u of 13.8 mm. Specimen M-8-2 exhibited an F_y of 21.4 kN and a δ_y of 8.8 mm, an F_{max} of 28.2 kN with a δ_u of 15.1 mm.

The results obtained from the experiment indicated that the average yield and ultimate capacities were 20.3 kN and 27.4 kN, respectively. Additionally, the average yield and ultimate slips were found to be 6.46 mm and 15.4 mm, respectively. The screws experienced a brittle mode of failure in both specimens, with the connectors breaking at the interface between the smooth and the threaded shank. The occurrence of panel crushing or splitting was minimal. The observed failure mode indicates that the response was governed by the strength of the connectors, rather than the timber.

The M-10 specimens demonstrated ductility, evidenced by the plastic hinges in the screws. Their secant stiffness $k_{0.4}$ and $k_{0.6}$ varied between 3.41–6.08 kN/mm. For specimen M-10-1, F_y was 33.2 kN, δ_y was 5.9 mm. Its F_{max} was 40.5 kN, and δ_u 24.8 mm. Its counterpart, Specimen M-10-2 had a F_y of 26.0 kN, a δ_y 7.5 mm and reached an F_{max} of 31.7 kN with a δ_u of 21.5 mm. On average, the specimens exhibited average F_y and F_{max} of 29.6 kN and 36.1 kN, respectively.

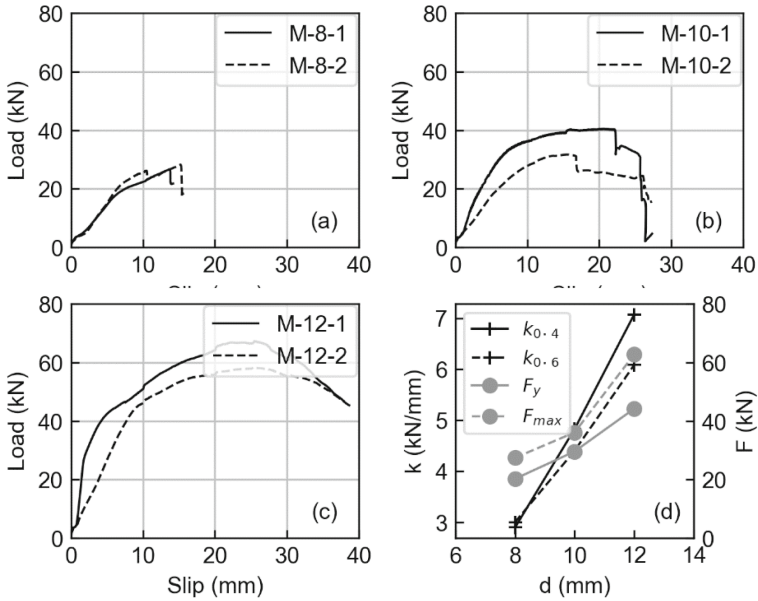


Fig. 4. Load-slip curves from monotonic tests for Specimens: a) M-8, b) M-10, c) M-12; d) the relationship between the screw diameter and stiffness and strengths.

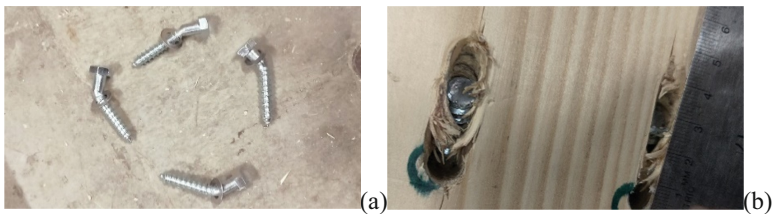
The average δ_y and δ_u were 6.7 and 23.2 mm, respectively. From the load-slip curves, it was evident that the connections exhibited an elastic-plastic behaviour, undergoing plastic deformation up to the point of failure. All screws had a plastic hinge indicating ductile forms of failure. For M-10-1 there was a notable timber compression where the split measured 17 mm from the initial screw axis to its ultimate position prior to failure.

The M-12 connections also exhibited a ductile response. Their secant stiffness varied between 5.28–8.87 kN/mm. For Specimen M-12-1, the F_y was 42.0 kN with an associated δ_y of 4.1 mm, while its F_{max} reached 67.2 kN at a δ_u of 34.4 mm. Meanwhile, Specimen M-12-2 presented an F_y of 42.0 kN at a δ_u of 4.1 mm, an F_{max} of 58.3 kN at a δ_u of 38.0 mm. The average F_y and F_{max} were 44.2 kN and 62.7 kN, respectively, whilst the average δ_y and δ_u were 6.5 mm and 36.2 mm, respectively.

As indicated by the F - δ relationships, the specimens predominantly exhibited an elastic-plastic behaviour. This is consistent with the test observations indicating the development of plastic hinge in the screws that remained embedded in the panel upon failure, which was more visible than that shown in the other tests. Comparatively to M-8 and M-10, more evident timber crushing occurred for these specimens. From Fig. 4d and Table 1 it is also shown that stiffness ($k_{0.4}$ and $k_{0.6}$), strengths (F_y and F_{max}), and slip ductility ratio (μ_δ) increase with screw diameter. Note that the bolded numbers in Table 1 and 2 represent the average values from two tests, followed by the standard deviation.

Table 1. Results from the monotonic tests.

Specimen	$k_{0,4}$ (kN/mm)	$k_{0,6}$ (kN/mm)	F_y (kN)	F_{max} (kN)	δ_y (mm)	δ_u (mm)	μ_δ (-)
M-8-1	2.85	2.92	19.10	26.62	6.50	13.77	2.12
M-8-2	2.94	3.08	21.40	28.20	6.80	15.10	2.22
M-8	2.89 ± 0.06	3.00 ± 0.11	20.25 ± 1.63	27.41 ± 1.12	6.65 ± 0.21	14.44 ± 0.94	2.17 ± 0.07
M-10-1	6.08	5.39	33.20	40.51	5.90	24.80	4.20
M-10-2	3.57	3.41	26.00	31.68	7.50	21.50	2.87
M-10	4.83 ± 1.77	4.40 ± 1.40	29.60 ± 5.09	36.10 ± 6.24	6.70 ± 1.13	23.15 ± 2.33	3.54 ± 0.95
M-12-1	8.87	6.84	42.00	67.17	4.10	34.40	9.20
M-12-2	5.28	5.33	46.40	58.30	8.90	38.00	4.27
M-12	7.07 ± 2.54	6.08 ± 1.07	44.20 ± 3.11	62.74 ± 6.27	6.50 ± 3.39	36.20 ± 2.55	6.73 ± 2.91

**Fig. 5.** a) Screws developing a plastic hinge, b) extent of damage in timber.

4.2 Reuse Potential Tests

Figure 6 shows the load-slip curves for the specimens tested under the reuse potential protocol, which included ten loading-unloading cycles, followed by disassembly, reassembly with new screws and testing to failure. The cyclic part of the protocol is denoted with (I), and the post-reassembly part with (II). In all situations the secant stiffness of the first cycles was lower than that of the subsequent nine cycles. This is evidenced in by the average $k_{I0,4}$ versus $k_{II0,4}$ in Table 2. The secant stiffnesses for the first cycle $k_{I0,4}$ were 4.15 kN/mm, 4.53 kN/mm and 5.98 kN/mm for the R-8, R-10, and R-12 specimens. The tenth cycle stiffnesses $k_{I0,4}$ were 8.34 kN/mm, 9.28 kN/mm, and 12.13 kN/mm for R-8, R-10, and R-12 elements, respectively. Figure 8a shows that $k_{I0,4}$ enhances after the first cycle, and then is relatively constant.

After disassembly, it was observed that most screws were slightly bent, and had signs of wear, especially on their threads, making them hard to remove. The steel section was largely intact. Figure 7 shows a representative screw and panel after disassembly, indicating permanent deformations at the screw and some ovalisation of the panel hole. The diameter of the hole following the loading direction was around 9 mm for the 8 mm screw, suggesting limited damage during the loading and unloading cycles. This is captured by a small translation of the unloading branch of the cycles in Fig. 6.

The installation of new screws did not have a significant effect on the elastic behaviour of the shear connection. As depicted in Table 2, the secant stiffness $k_{II0,4}$ was within similar ranges to $k_{I0,4}$. For the R-8, R-10, and R-12 specimens, $k_{II0,4}$ was 17.3%, 16.8%,

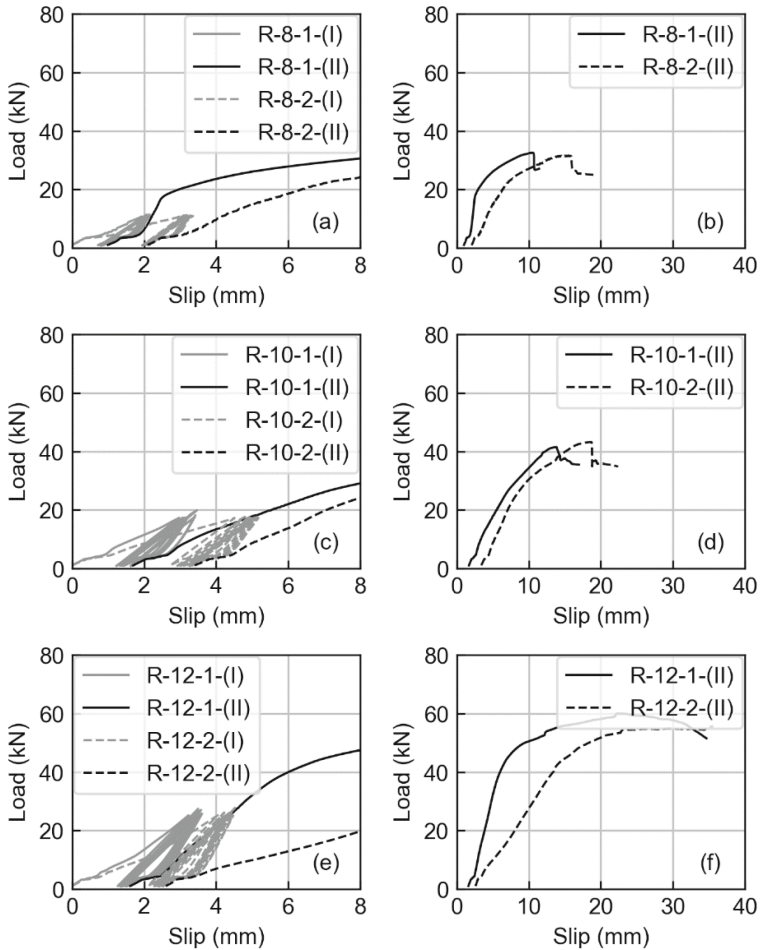


Fig. 6. Load-slip curves for: R-8 specimens a) cyclic tests (I), b) monotonic tests (II); R-10 specimens c) cyclic tests (I), d) monotonic tests (II); R-12 specimens e) cyclic tests (I), f) monotonic tests (II).

and 7.7% higher than $k_{I0.4}$. These values are within the standard deviation of the tests, thus can be considered insignificant. The $k_{II0.6}$ suggests similar observations. With regard to the strengths, for the R-8, R-10, and R-12 groups, the average F_y were 23.8 kN, 25.3 kN and 48.1 kN, respectively. For the same groups, the average F_{max} were 32.1 kN, 42.4 kN, and 57.9 kN, respectively. These values are similar to and within the standard deviation of those from the monotonic tests presented in Table 1.

It is shown that the disassembly and reassembly had minimal or no influence on the strength and stiffness, indicating full reusability of the CLT panels. With regard to ultimate displacement δ_u and slip ductility μ_δ , the differences between the samples under the monotonic tests and reuse potential tests are also rather minor. For M-8 $\mu_\delta = 2.2$, whilst for R-8 $\mu_\delta = 3.1$; for M-10 $\mu_\delta = 3.5$, whilst for R-10 $\mu_\delta = 3.5$; and for M-12 μ_δ

Table 2. Results from the reuse potential tests.

Specimen	$k_{I,0.4}$ (kN/mm)	$k_{I,0.4}^*$ (kN/mm)	$k_{II,0.4}$ (kN/mm)	$k_{II,0.6}$ (kN/mm)	F_y (kN)	F_{max} (kN)	δ_y (mm)	δ_u (mm)	μ_δ (-)
R-8-1	3.28	9.02	5.02	4.72	23.50	31.57	4.80	13.81	2.88
R-8-2	5.02	7.65	-	-	24.00	32.54	3.10	9.73	3.14
R-8	4.15 ± 1.24	8.34 ± 0.97	5.02 ± 0.00	4.72 ± 0.00	23.75 ± 0.35	32.06 ± 0.69	3.95 ± 1.20	11.77 ± 2.88	3.01 ± 0.19
R-10-1	5.50	9.68	5.48	5.00	23.50	41.49	3.95	15.24	3.86
R-10-2	3.57	8.89	5.42	5.11	27.00	43.21	4.81	15.10	3.14
R-10	4.53 ± 1.36	9.28 ± 0.56	5.45 ± 0.04	5.06 ± 0.08	25.25 ± 2.47	42.35 ± 1.22	4.38 ± 0.61	15.17 ± 0.10	3.50 ± 0.51
R-12-1	5.97	11.82	8.96	9.41	47.20	59.94	5.03	33.03	6.57
R-12-2	5.98	12.45	4.00	3.72	49.00	55.90	12.80	43.50	3.40
R-12	5.98 ± 0.01	12.13 ± 0.45	6.48 ± 3.50	6.57 ± 4.03	48.10 ± 1.27	57.92 ± 2.86	8.92 ± 5.49	38.26 ± 7.40	4.98 ± 2.24

= 6.7, whilst for R-12 $\mu_\delta = 5.0$. As for the other parameters, the difference in ductility parameters between the two sets of tests were within the standard deviation.

Considering the potential for reusing and recycling steel and timber in construction, it is apparent that the steel sections can be repurposed effectively. In this particular case, as there was no visible damage to the steel section, the same holes were used. However, other areas can be targeted for drilling, away from the previously used points, if needed.

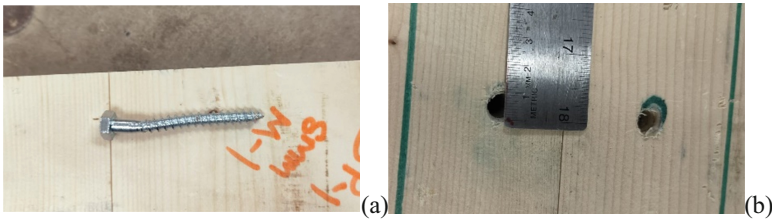


Fig. 7. Details after disassembly: a) deformed screw, b) timber hole ovalisation.

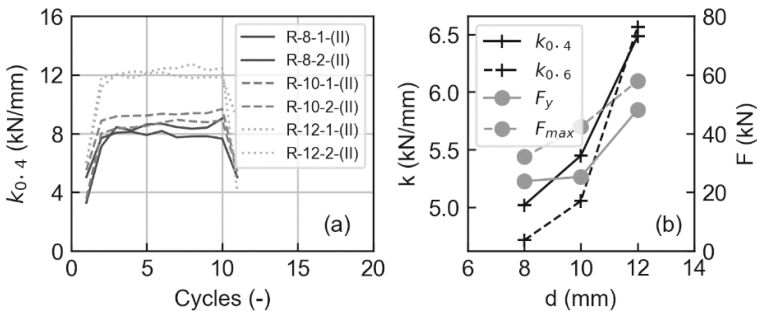


Fig. 8. a) Stiffness response of reuse potential test specimens, b) relationship between screw diameter versus stiffness and strength from the monotonic tests (II) for R specimens.

As for the CLT panels, they offer multiple ways for reuse. One option is to flip and interchange the panel sides, while another is to introduce screws at points more than 100 mm away from previous screw locations, as these would be far away from the damaged areas due to loading. From the test observations, it is worth noting that reusing the screws for different specimens is not possible as these had hinging and straightening would change the mechanical properties.

In lack of guidance for the evaluation of the reuse potential of steel-timber shear connection components, a procedure was adopted involving ten loading-unloading cycles to 40% of the failure load of the monotonic testing counterpart specimens. Although the loading regime is representative only for some in-service loading scenarios, the lower amplitude and higher number of cycles obtained from a probabilistic approach for the load distributions and changes during the design life of a building could be considered. The approach assumed only short-term loading, which does not include specific material effects such as creep in timber, which may change the overall structural response and CLT reuse potential.

The paper showed that dry connections using coach screws enable component disassembly of steel-timber hybrid systems at the end of life, rendering them circular. For quantification of reuse potential, a structural reuse index can be developed using quantitative information obtained from the testing, such as the relative stiffness between the reassembled and original specimen, the relative load-carrying capacity of the reassembled specimen and that tested under monotonic conditions, the permanent deformations in the removed screws, as well as qualitative parameters related to the user perception on the disassembly process. This index can be incorporated or correlated with typical circularity indicators for buildings.

5 Concluding Remarks

This paper evaluated the disassembly capability of steel-timber shear connections, tested under in-service cyclic loading, as well as their reassembly and structural reuse potential through testing. A detailed account of experiments involving double shear configurations with coach screws of three diameters (8, 10, 12 mm) was given. Monotonic tests were first carried out to evaluate the main mechanical response parameters. Counterparts were then tested under ten loading-unloading cycles to 40% of the capacity obtained from monotonic tests to evaluate stiffness degradation characteristics as well as specimen kinematics. After disassembly and measurements, the specimens were reassembled and tested to failure. The main remarks are outlined below.

The monotonic tests showed that the secant stiffnesses, yield and ultimate strengths, and slip ductility ratios increase with screw diameter, as expected. The 8 mm screws experienced a brittle failure at the interface between the smooth shank and the threaded shank, whilst CLT panel crushing or splitting was minimal. The 10 mm and 12 mm screws had a plastic hinge indicating ductile forms of failure.

The cyclic test observations indicated that the secant stiffness increased after the first cycle, and then was relatively constant to the tenth cycles for all specimens. After disassembly, all screws, regardless of their size, had permanent deformations, and the timber panel indicated limited damage during the loading-unloading cycles, in the range

of 1 mm. The stiffness, strength and ductility of the reassembled specimens were similar to those from the monotonic tests.

The disassembly and reassembly had minimal or no influence on the strength and stiffness, indicating full reusability of the CLT panels. For quantification of the reuse potential, a structural reuse index can be developed using quantitative measurements from the tests. This index can then be incorporated or correlated with commonly used circularity indicators for buildings.

References

1. Spear M, Hill C, Norton A, Price C, Ormondroyd G (2019) Wood in construction in the UK. Report
2. Stepinac M, Šušteršič I, Gavrić I, Rajčić V (2020) Seismic design of timber buildings: highlighted challenges and future trends. *Appl Sci* 10(4):1380
3. Offerman T, Bompá DV (2023) Numerical investigation of lateral behaviour of steel-timber hybrid frames. *ce/papers* 6(3–4):470–476
4. Loss C, Piazza M, Zandonini R (2016) Connections for steel-timber hybrid prefabricated buildings. Part II: innovative modular structures. *Const Build Mat* 122:796–808
5. Karagiannis V, Málaga-Chuquitaype C, Elghazouli AY (2017) Behaviour of hybrid timber beam-to-tubular steel column moment connections. *Eng Struct* 131:243–263
6. Hassanieh A, Valipour HR, Bradford MA (2016) Experimental and numerical study of steel-timber composite (STC) beams. *J Constr Steel Res* 122:367–378
7. Bompá DV, Dance G, Chira A, Walker MG, Nagy Z (2023) Structural response of hybrid timber-cold formed steel floors. *ce/papers* 6(3–4):1853–1858
8. Asiz A, Smith I (2011) Connection system of massive timber elements used in horizontal slabs of hybrid tall buildings. *J Struct Eng* 137(11):1390–1393
9. Wang CL, Lyu J, Zhao J, Yang H (2020) Experimental investigation of the shear characteristics of steel-to-timber composite joints with inclined self-tapping screws. *Eng Struct* 215:110683

Open Access This chapter is licensed under the terms of the Creative Commons Attribution 4.0 International License (<http://creativecommons.org/licenses/by/4.0/>), which permits use, sharing, adaptation, distribution and reproduction in any medium or format, as long as you give appropriate credit to the original author(s) and the source, provide a link to the Creative Commons license and indicate if changes were made.

The images or other third party material in this chapter are included in the chapter's Creative Commons license, unless indicated otherwise in a credit line to the material. If material is not included in the chapter's Creative Commons license and your intended use is not permitted by statutory regulation or exceeds the permitted use, you will need to obtain permission directly from the copyright holder.

